

Contents lists available at [ScienceDirect](https://www.sciencedirect.com)

Case Studies in Construction Materials

journal homepage: www.elsevier.com/locate/cscm

Strengthening of reinforced concrete beams without transverse reinforcement by using intraply hybrid composites

ARTICLE INFO

Keywords

Reinforced concrete beams
 Intraply hybrid composites
 U-shape strengthening
 Aramid-carbon (AC) hybrid composite
 Glass-aramid (GA) hybrid composite
 Carbon-glass (CG) hybrid composite

ABSTRACT

Concrete is currently among the most widely used materials all around the world. The main advantages of concrete include durability, versatility, and high compressive strength, but significant disadvantages include low tensile strength, low shear strength, and low ductility. To eliminate these disadvantages, longitudinal and transverse reinforcements are usually preferred. Steel is widely used as a reinforcement material in the world, but there is still research underway to find alternative materials. In recent decades, composite materials have been used to reinforce concrete instead of steel materials. This study focuses on Intraply Hybrid Composites (IHCs), which are had an important place in the composite industry and examines how these composites affect concrete beams as far as their shear strength is concerned. For this purpose, A length of 2 m RC beams, with no transverse reinforcement (RC2.0), is prepared and then reinforced with three IHCs, Aramid-Carbon (AC2.0), Glass-Aramid (GA2.0) and Carbon-Glass (CG2.0). After U-shape strengthening, the specimens are inspected in four-point bending tests and the effects of the IHCs are investigated on the shear strength of the beams. The experimental results show that there is an increase of 4.36%, 10.62%, and 15.28% in the ultimate load capacity of AC2.0, CG2.0, and GA2.0, respectively, compared to reference specimen, RC2.0. Furthermore, the type of hybrid composite has a direct impact on the failure modes of the RC beams. Consequently, the IHCs can provide a significant contribution to the structural behavior of RC beams.

1. Introduction

The construction industry has been using concrete for centuries and it is still the preferred material for most of the world's buildings. In addition to having many advantages, such as high compressive strength, easy production and application, durability, and accessibility, concrete also has some drawbacks, such as low tensile strength and low shear strength. As a result of these disadvantages, concrete is typically reinforced with steel bars, followed by concrete being converted to reinforced concrete (RC). Although steel rebars are widely used as reinforcement material throughout the world, research is still being conducted to find alternatives. Fiber reinforced polymer (FRP) materials, one of the fastest growing groups of materials in recent years, have recently begun replacing steel rebars as a significant alternative material. Technically, FRPs are composite materials made with polymers and fibers [1]. As FRPs have remarkable properties such as high mechanical performance, low density, high chemical resistance, high thermal performance, high corrosion resistance, and high energy absorption, they have great potential in many fields [2,3]. Therefore, FRPs have become extremely important in many engineering applications. They're available for a wide range of uses [4–8]. Researchers have also examined the feasibility of using FRP to improve the shear strength of RC beams. For example, Spinella [9] studied the effective failure strain of FRP reinforcement. It was noted that internal and external reinforcements contribute to the shear strength of a beam in relation to its axial rigidity. In another study, an experimental study was conducted by Colalillo and Sheikh [10] to investigate behavior of shear-critical RC beams strengthened with FRP composites. The study also showed that FRP strengthening was effective at improving shear performance of the RC beams. Bousselham and Chaallal (2013) [11] investigated the impact of the CFRP on the RC beams. It was determined that the use of CFRP has significant effects on the shear strength of the RC beams. Similarly, Zhang and Hsu [12] focused on the shear strengthening of RC beams using carbon FRP (CFRP) laminates. The study concluded that the epoxy-bonded CFRP increases the load-carrying and shear capacities of the RC beams.

<https://doi.org/10.1016/j.cscm.2021.e00700>

Received 24 May 2021; Received in revised form 28 August 2021; Accepted 13 September 2021

Available online 20 September 2021

2214-5095/© 2021 The Author(s). Published by Elsevier Ltd. This is an open access article under the CC BY-NC-ND license

(<http://creativecommons.org/licenses/by-nc-nd/4.0/>).



Fig. 1. Preparation of the RC Beams (a) Placing strain gauges on the rebars, (b) Wooden molds, (c) Placing the rebars in the mold, (d) Concrete from a concrete plant.

FRPs have evolved into many types in recent years depending on their manufacturing processes and materials. Intraply Hybrid Composites (IHCs) are among the most popular FRPs [13,14]. In technical terms, IHC refers to a composite layer consisting of two or more fibers oriented in different directions within a single matrix and IHCs have been studied by a range of researchers in recent years. For example, Zhao et al. [15] investigated the impact behavior and damage mechanism of novel carbon dyneema hybrid fabric reinforced plastic composites using drop weight and steel ball impact tests. Hashim et al. [16] studied the carbon-Kevlar reinforced epoxy hybrid composites and the effect of fiber loading directions on the fatigue of the hybrid composites at low cycles. Rajasekar et al. [17] evaluated the mechanical properties such as tensile strength, elastic modulus, flexural strength, and flexural modulus of intraply carbon aramid hybrid composite laminates. Yang et al. [18] conducted experimental and numerical tests to investigate the hybridization effect on the composites under impact velocity based on fabrics and polymerized poly (butylene terephthalate) resin. Dehkordi et al. [19] focused on the effect of hybridization on the impact behavior and residual compressive strength of intraply basalt/nylon hybrid composites.

Recent studies have examined the mechanical and physical properties of IHCs, but there has been no research on their use in civil engineering or construction. Due to this, the present study represents an important contribution to the field of IHCs used as reinforcing materials for construction. It is the main aim of this study to investigate the behavior of IHC reinforced beams and to investigate how different types of IHCs influence structural performance. Two-meter lengths of RC beams without transverse reinforcement were prepared and reinforced with monolayer IHCs with 0.2 mm thickness and 200 g per square meter (GSM). In this study, Aramid-Carbon (AC), Glass-Aramid (GA) and Carbon-Glass (CG), supplied by CARBOMID textile company (Istanbul, Turkey), were chosen as IHCs. Moreover, the specimens were subjected to four-point bending tests considering the ratio of shear span (a) to effective depth (d) equals 3 ($a/d=3$) and the effects of the IHCs on the shear strength of the beams were investigated.

2. Materials and methods

2.1. Preparation of the RC beams

As a first step, wooden molds were prepared with 15 mm plywood and the molds were cleaned with water. Then, the inner surfaces

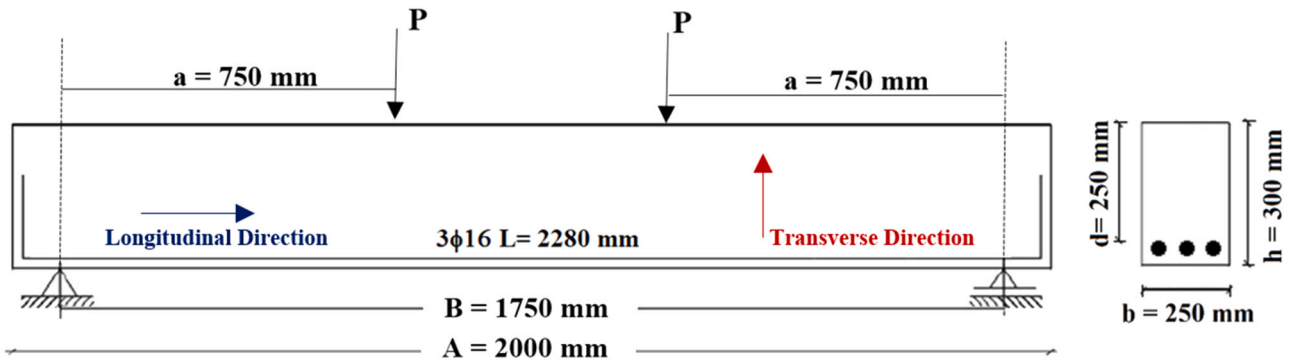
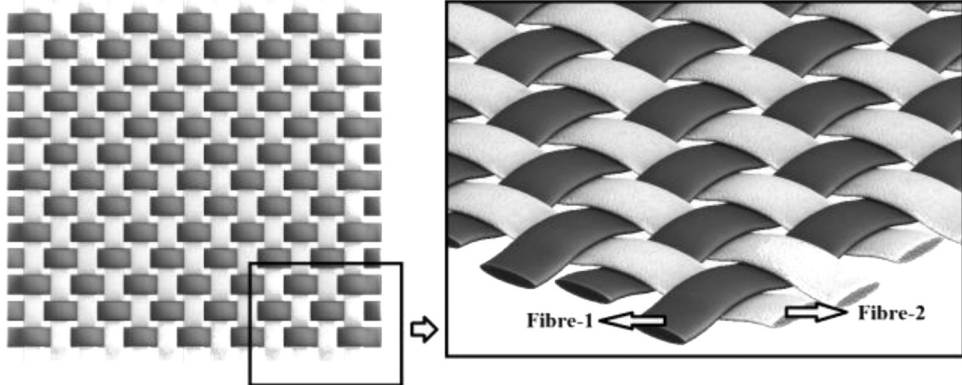
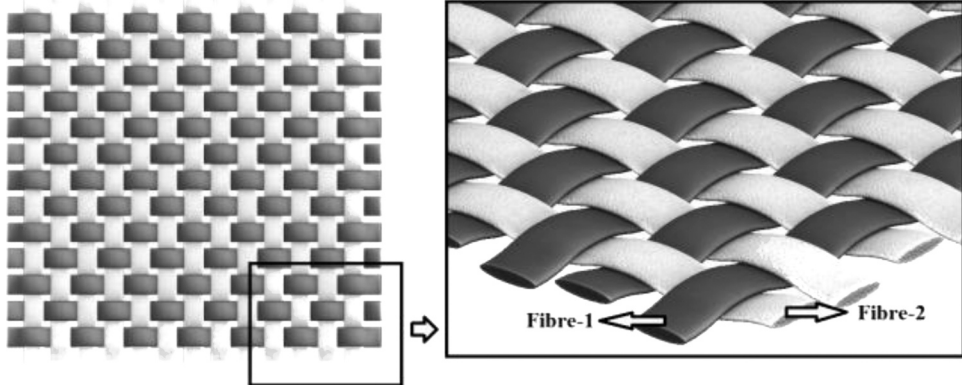


Fig. 2. Geometric sizes and reinforcement layout of the beams.

Table 1
Strengthening information of the beams.

Parameters		Specimens			
		RC2.0	AC2.0	GA2.0	CG2.0
Geometric Information	$b/h/d$ (mm/mm/mm)	250/300/250	250/300/250	250/300/250	250/300/250
	(a/d) (mm/mm)	750/250 = 3	750/250 = 3	750/250 = 3	750/250 = 3
Material Properties	f_c (MPa)	41.6	41.6	41.6	41.6
	f_y/f_{su} (MPa)	502/642	502/642	502/642	502/642
	$\epsilon_{sh}/\epsilon_{su}$	0.009/0.14	0.009/0.14	0.009/0.14	0.009/0.14
Longitudinal Reinforcement	flexural reinforcement (ratio)	3 ϕ 16 (0.0093)	3 ϕ 16 (0.0093)	3 ϕ 16 (0.0093)	3 ϕ 16 (0.0093)
Intraply Hybrid Composites (IHCs)	Transverse:	–	Aramid	Glass	Carbon
	Longitudinal:	–	Carbon	Aramid	Glass
	Schematic of a monolayer IHC				



f_c = The specified compressive strength of concrete.
 f_y = The yield strength of rebar.
 f_{su} = The ultimate strength of rebar.
 ϵ_{sh} = The strain at the onset of strain hardening for rebar.
 ϵ_{su} = The ultimate strain limit for rebar.



Fig. 3. Strengthening of the Beams with the IHCs (a) Cutting IHCs with electric scissor, (b) Applying a thin coat of adhesive material, (c) Application of the IHC, (d) Applying the adhesive material on the surfaces of the IHC.

were coated with oil to easily separate and demould the hardened beam specimens. Next to oiling the molds, three $\phi 16$ -standard rebars were placed longitudinally in the molds, and three different strain gages were installed in each rebar. Concrete from a concrete plant was poured into molds using a concrete vibrator (Fig. 1). Subsequently, the surfaces were smoothed, and the specimens were cured in the laboratory environmental conditions. After 24 h of curing, the molds were carefully removed, and the specimens were cured until the test day in the laboratory. The geometrical properties of the beams are shown in Fig. 2.

2.2. Strengthening configurations

Before applying the IHCs, the rough surfaces of the RC beams were sanded, and the corners were beveled to remove the negative effects of the corners. To remove any contaminants, the surfaces were cleaned with water and acetone. Afterward, the composites were cut with electric scissor according to the size required, and epoxy resin was used to prepare the adhesive (Duratek AV 21 with resin/hardener ratio 100:27, as specified by the manufacturer). Following uniform mixing of the adhesive material, a thin coat of adhesive material was applied to the surfaces of the beams using a roller brush. After that, the IHCs were carefully applied to the beam surfaces and the adhesive material was applied to the composite surfaces. After applying IHCs, the reinforced beams were cured for ten days in the laboratory. As reinforcement configurations, Aramid-Carbon (AC2.0), Glass-Aramid (GA2.0) and Carbon-Glass (CG2.0) hybrid composites were preferred (Table 1).

Strengthening of a beam is usually limited to three sides in most circumstances. Due to inaccessibility of the upper cross section, U-

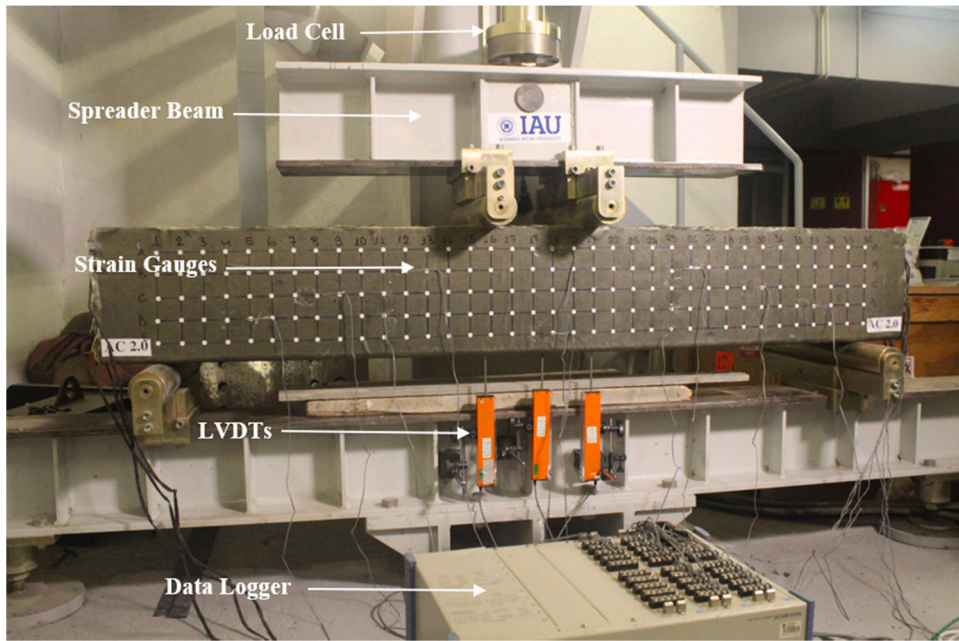


Fig. 4. Experimental setup.

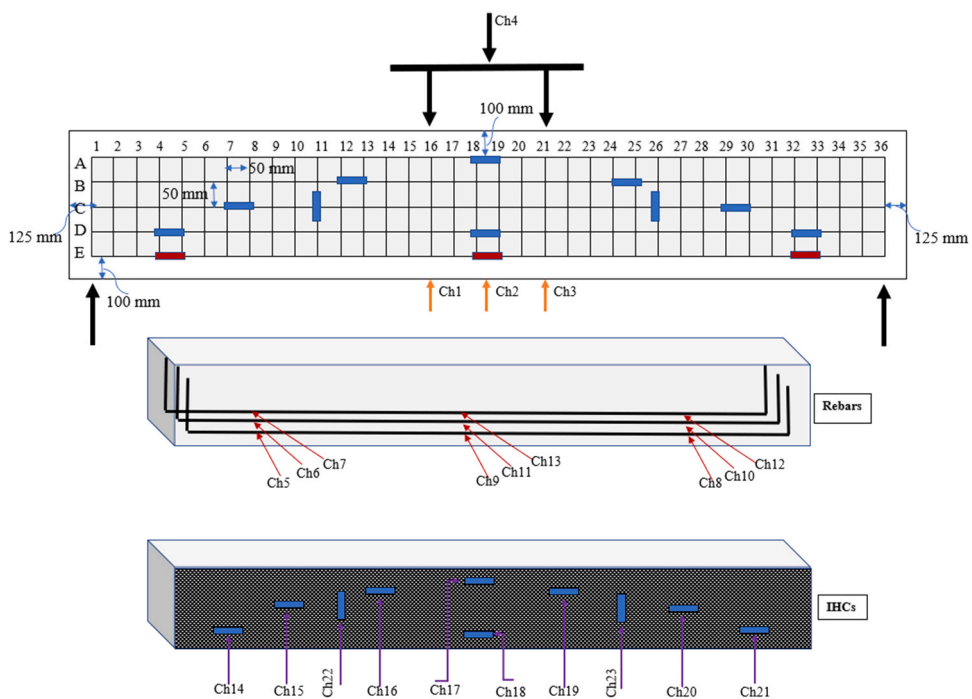


Fig. 5. Layout of the instruments.

shaped reinforced structures (three sides) are more practical for beam-slab construction. Moreover, the literature discusses the effect of strengthening with fiber reinforced polymer (FRP) composite materials on four sides versus three sides of the beams [20,21]. According to previous studies, the beams strengthened on four sides and three sides with FRP composite materials exhibited similar behavior. Therefore, the IHCs were applied to three surfaces of the beam specimens (U-shaped reinforcement) shown in Fig. 3.

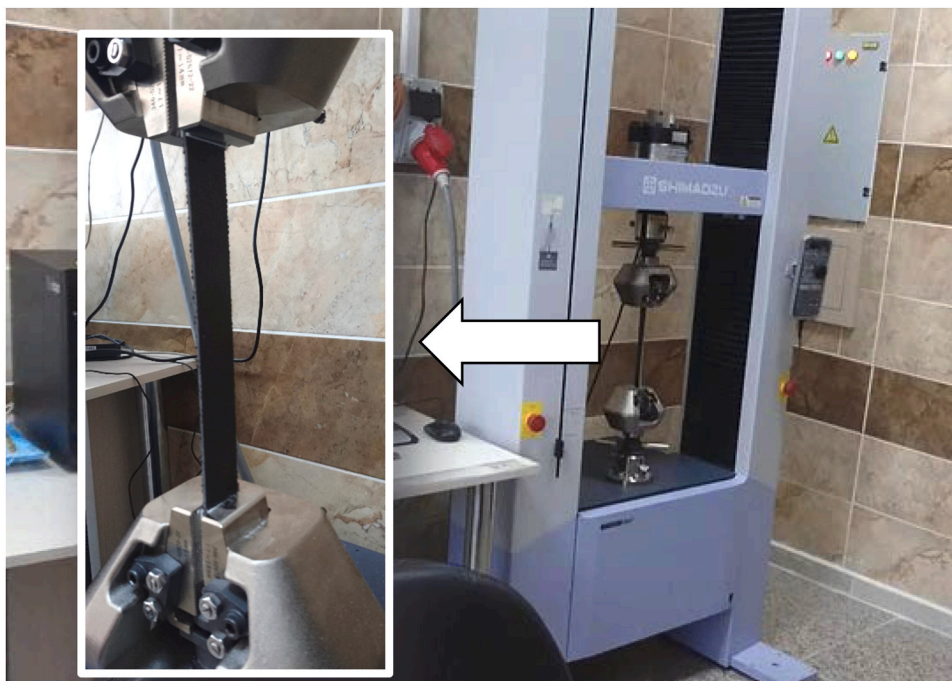


Fig. 6. Tensile tests of the IHCs.

Table 2

Mechanical properties of the IHCs.

Specimen	Direction	Tensile Strength (MPa)	Young Modulus (GPa)	Density (g/cm^3)
AC	Longitudinal	143.95 ± 10.15	88.71 ± 6.37	1.37
	Transverse	107.29 ± 6.45	68.23 ± 4.24	
GA	Longitudinal	131.02 ± 13.86	72.42 ± 6.06	1.43
	Transverse	71.28 ± 6.69	51.39 ± 4.45	
CG	Longitudinal	55.06 ± 3.52	44.66 ± 2.84	1.59
	Transverse	145.52 ± 21.98	101.47 ± 1.68	

2.3. Instrumentation and testing procedure

To investigate the behavior of the tested specimens, the applied load, strains in the rebars and composites, and displacements of the beams were recorded using load cells (Ch4), strain gages, and Linear Variable Differential Transformers (LVDTs), respectively. The rebars were monitored with nine strain gauges (Ch5–13) with three strain gauges per rebar. Nine strain gauges were also used to monitor the IHCs, six of them lateral (Ch15–21) and two verticals (Ch22 and Ch23). On the underside of each beam, three LVDTs were placed: one at the mid-span (Ch2), two at the half-span (Ch1 and Ch3) to monitor the vertical deflection during testing. During the tests, a video camera was also used for visual inspection. A data logger continuously recorded the data from the devices. Fig. 4 illustrates the experiment setup and Fig. 5 shows all of the devices configured in detail.

3. Experimental program

The experimental program was divided into two phases. In the first stage, the materials used in the study were characterized to determine their mechanical properties. In the second stage, four-point bending tests were performed on the beam specimens to observe the contribution of the IHCs on the shear performance of the beams.

3.1. Characterization of the materials

3.1.1. Mechanical properties of the IHCs

The monolayer IHCs were tested on specimens with lengths of 250 mm and widths of 25 mm, and the fiber weight fractions of GA, AC, and CG hybrid composites were 51%, 53%, and 58%, respectively. The tensile testing was performed with a universal mechanical testing machine equipped with a 100 kN load cell according to ASTM D3039/D3039M-17 [22]. The tensile testing apparatus is



Fig. 7. Compression tests of the concrete samples.

Table 3
Mechanical properties of the concrete samples.

Properties	Value
Compression strength (MPa)	41.60 ± 0.871
Young modulus (MPa)	17,401 ± 89.2
Poisson's ratio	0.161 ± 0.007
Tangent modulus (MPa)	23,190
Secant modulus (MPa)	17,396



Fig. 8. Tensile test of the rebar.

Table 4

The mechanical properties of the rebars.

Samples	Mass (kg/m)	Yield load (kN)	Yield strength (MPa)	Tensile strength (MPa)	Breaking strain (%)
1	1.572	101.000	502.000	643.000	16.900
2	1.570	99.200	493.000	640.000	17.700
3	1.550	103.000	512.000	641.000	15.400
Average	1.564	101.067	502.333	641.333	16.667
Std.Dev.	0.012	1.901	9.504	1.528	1.168

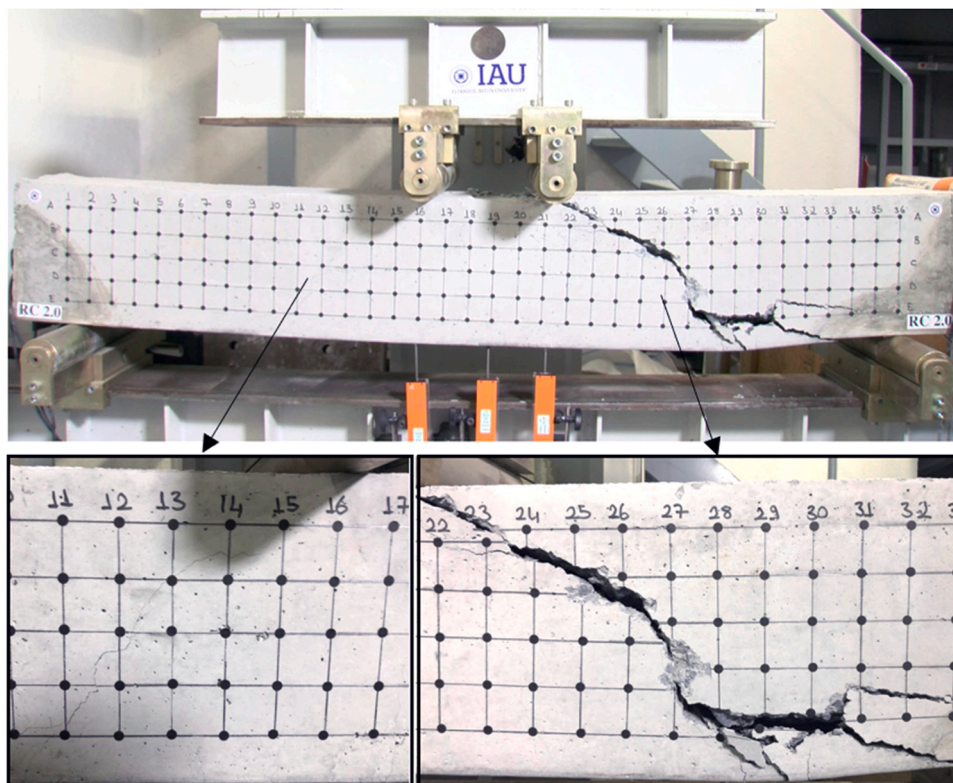


Fig. 9. Typical failure pattern of the reference sample (RC2.0).

illustrated in Fig. 6. The density measurements of the composites were carried out as per ASTM D792–20 [23]. The mechanical properties obtained during the tests are summarized in Table 2.

3.1.2. Mechanical properties of the concrete

In this study, the beams were constructed with concrete of class C40 which has characteristic compression strength between 40 MPa and 44 MPa on the 28th day. To understand whether the concrete was of the desired quality, cylindrical test samples with a diameter of 150 mm and a height of 300 mm were taken during the construction of the beams. These test samples were cured under the same conditions as the beams. After 28 days, the cylindrical samples were tested mechanically in order to evaluate the accuracy of the concrete class and, more importantly, to determine its mechanical properties. The specimens were evaluated with direct compression tests according to BS EN 12390–3:2019 [24] and BS EN 206:2013+A2:2021 [25]. During the compression tests, a cylinder extensometer was also used to determine the Young modulus, Poisson's ratio, Tangent modulus and secant modulus of the concrete specimens according to ASTM C469/C469M [26] and BS EN 12390–5:2019 [27], BS EN 12390–13 [28] (Fig. 7). The mechanical properties of the material obtained from the experimental tests are presented in Table 3.

3.1.3. Mechanical properties of the rebars

In the construction of the reinforced concrete beams, $\phi 16$ rebars were used in the lower part of the beams to strengthen the beams longitudinally. Tensile tests were carried out on the rebars to determine the strength properties according to ISO 15630–1:2019 [29] and ISO 6892–1:2019 [30] as part of the experimental program (Fig. 8). Additionally, an elongation at break (%) measure was performed on the specimens with a strain transducer attached to each rebar. The mechanical properties of the specimens determined during the tests are shown in Table 4.

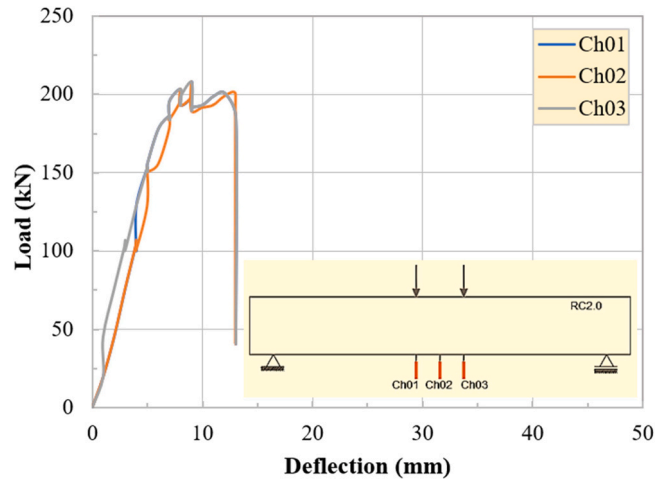


Fig. 10. Load-deflection curves of the RC2.0 beam.

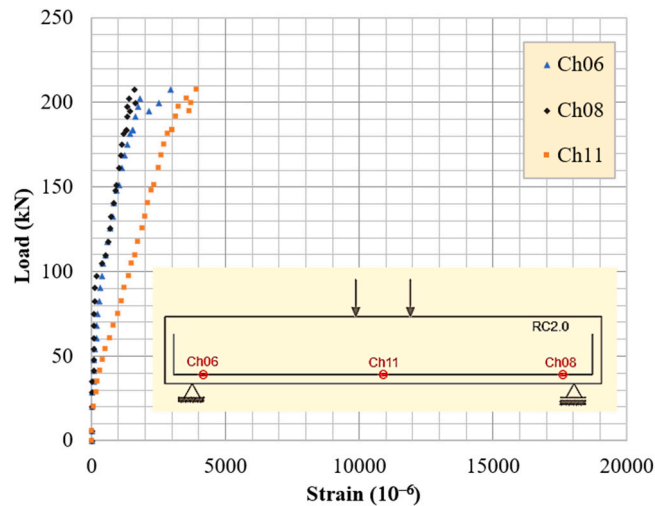


Fig. 11. Load-strain curves obtained from the rebars of the RC2.0 beam.

3.2. Four-point bending tests

Four-point bending tests were conducted on the beams in compliance with BS EN 12390-5 [31] following characterization of each material. Tests were controlled by displacements with a hydraulic actuator that can handle a maximum load of 500 kN and is located in the Department of Civil Engineering Laboratory at Istanbul Aydin University. In these tests, the top of the specimen was applied two equal vertical loads, and the tests were stopped when the specimen could no longer carry the load.

3.2.1. Reference sample (RC2.0)

In the first step, the reference RC beam without transverse reinforcement (RC2.0) was tested. During the test, a first crack became visible at nearly 160 kN in the middle of the span. A yielding of the longitudinal steel bars was observed at 170 kN using strain gauges. By increasing the load, the shear crack formed at 185 kN in the middle of the left shear field. When the load reached 200 kN, a second shear crack appeared in the middle of the right shear field. At 207.526 kN, RC2.0 failed due to reaching the shear strength on the right side of the beam (Fig. 9). The load-deflection curves displayed in Fig. 10 were derived from the LVDTs. Also, the curves for load-strain for rebars are shown in Fig. 11.

3.2.2. Aramid – carbon reinforced beam (AC2.0)

Test of the AC2.0 was performed after the RC2.0 test in the experimental program. First cracks appeared at 190 kN, due to the bending stress, in the middle of the span. The crack continued to widen as the load was increased. In the upper part of the beam, compression cracks were observed after the load was increased to 210 kN and the crack became more noticeable in the middle of the

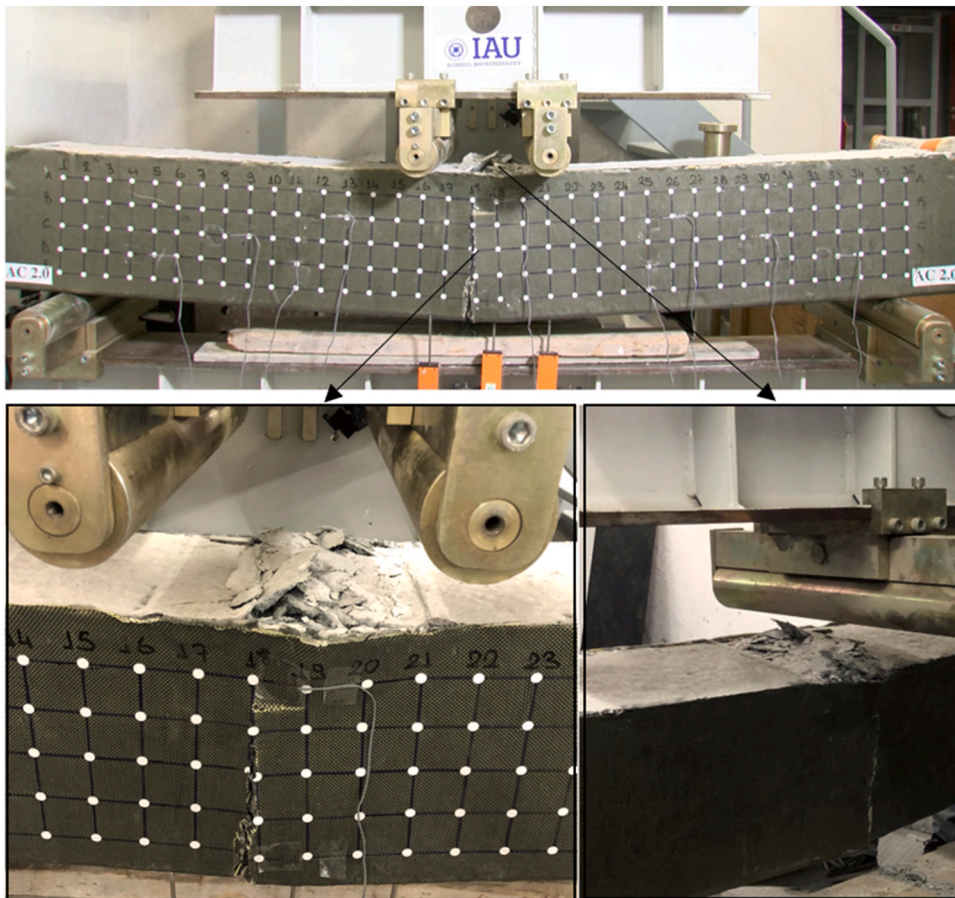


Fig. 12. Crack patterns and failure mode of the AC2.0.

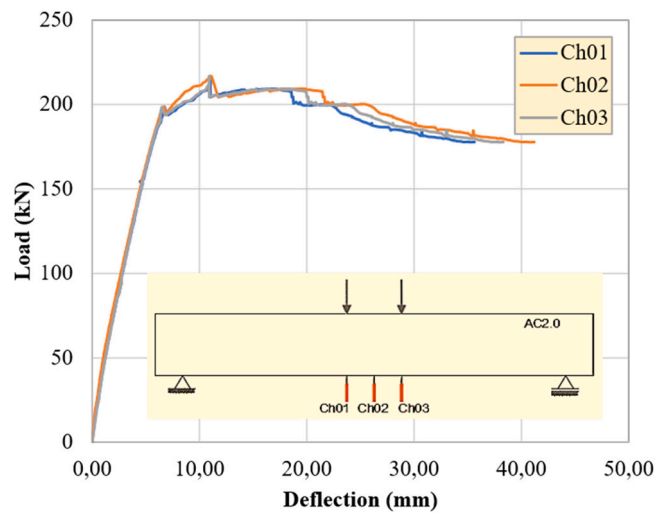


Fig. 13. Load-deflection curves of the AC2.0 beam.

span. In flexural testing, the AC2.0 failed when a maximum load of 216 kN was applied (Fig. 12). When the load was applied to the maximum, the deflection reached 40.2 mm. The curves for the load-deflections obtained from the LVDTs are displayed in Fig. 13. Figs. 14 and 15 illustrate, respectively, the curves obtained from the rebars and the AC-IHC.

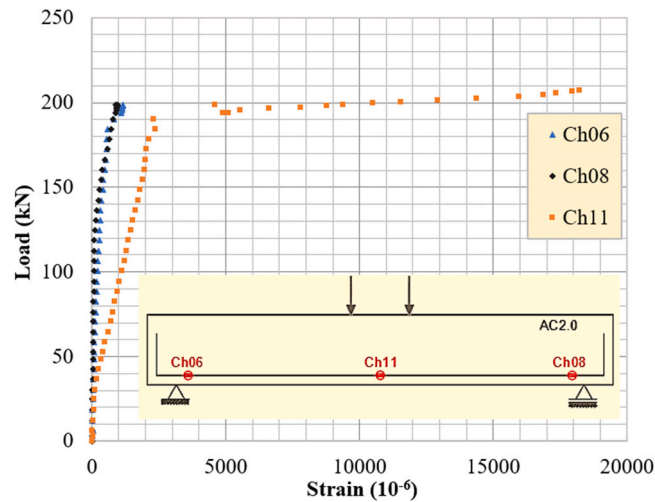


Fig. 14. Load-strain curves obtained from the rebars of the AC2.0.

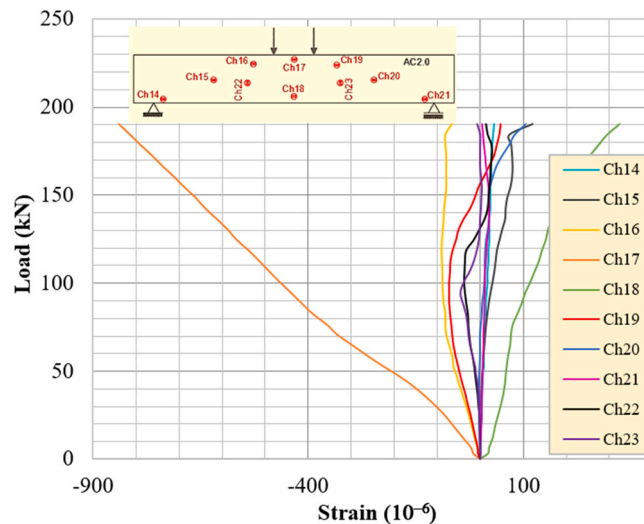


Fig. 15. Load-strain curves obtained from the AC-IHC.

3.2.3. Glass – aramid reinforced beam (GA2.0)

As part of the test program, the GA2.0 was tested at the third stage. At any point on the beam, no cracking was observed up to 200 kN of load. Strain gauges clearly demonstrated that the longitudinal steel rebar yields under a load of 210 kN. After 225 kN of load was applied to the beam, a hairline crack appeared near the center. In the left region of the beam, a shear crack formed as a result of increasing load. At 239 kN, the GA2.0 failed due to the occurrence of a crack related to shear fracture (Fig. 16). A maximum deflection of 11.04 mm was observed at the maximum load. A load-displacement curve obtained through the LVDTs is shown in Fig. 17. Moreover, the load-strain curves for the rebars and for the GA-IHC are shown in Figs. 18 and 19, respectively.

The longitudinally placed strain gauges Ch22 and Ch23 in Fig. 19 showed very high strain measurements. This is mainly a result of the strain gauges being situated near shear cracks. While the strains recorded in the strain gauges at this location are low in the specimens collapsing due to bending stresses, it is noteworthy that high strains are obtained in this beam collapsing due to shear stresses.

3.2.4. Carbon – glass reinforced beam (CG2.0)

Testing of the CG2.0 was conducted at the end of the experimental program. During loading, the first crack appeared in the middle of the beam as a flexural crack when the load reached 220 kN. As soon as the load level reached 224 kN, the load level dropped to 204 kN. In response to increasing the loading, the first crack suddenly widened, and a second flexural crack was visible nearby. With a load of about 220 kN, a new flexural crack developed near the center of the beam. As the load increased to about 225 kN, three cracks appeared in the beam, and it failed in flexure at 229 kN (Fig. 20). A maximum deflection of 39.76 mm was measured at failure (Fig. 21).

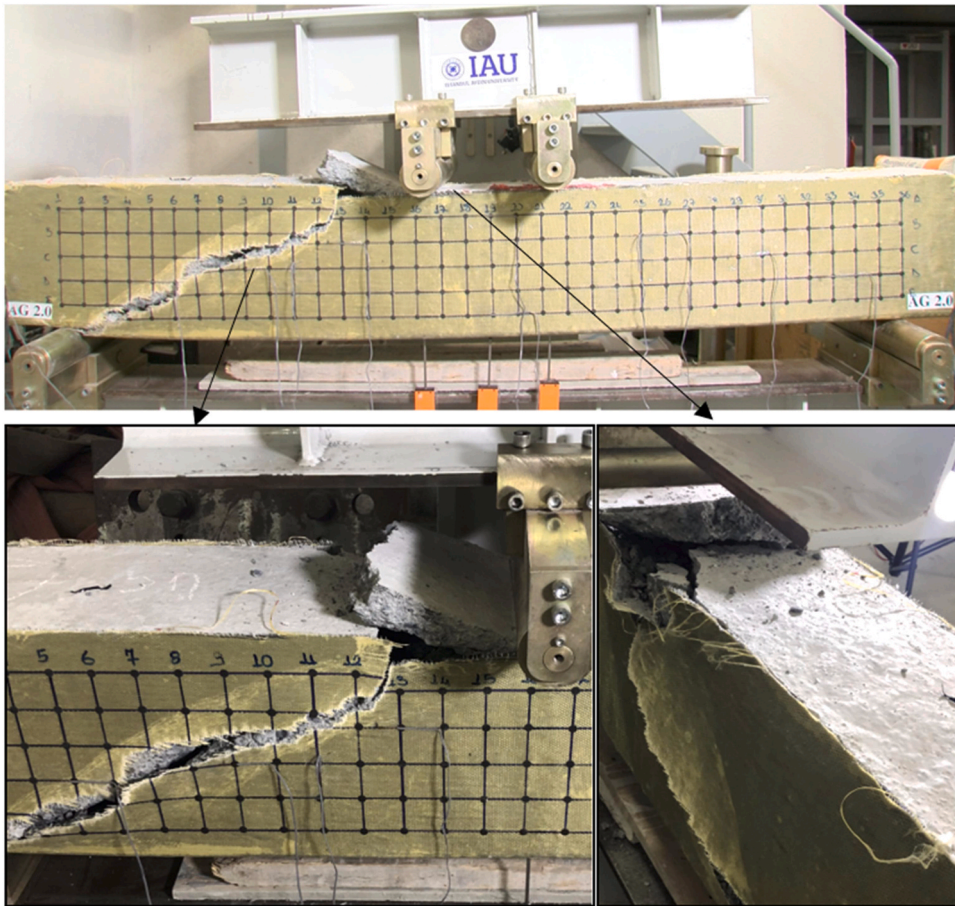


Fig. 16. Crack patterns and failure mode of the GA2.0.

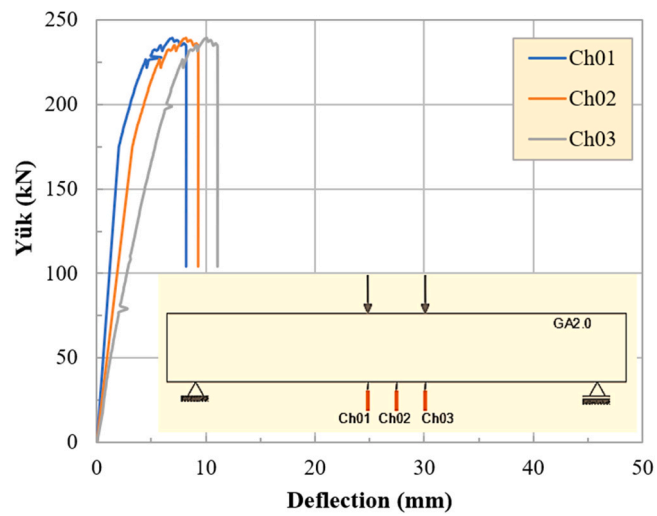


Fig. 17. Load-deflection curves of the GA2.0 beam.

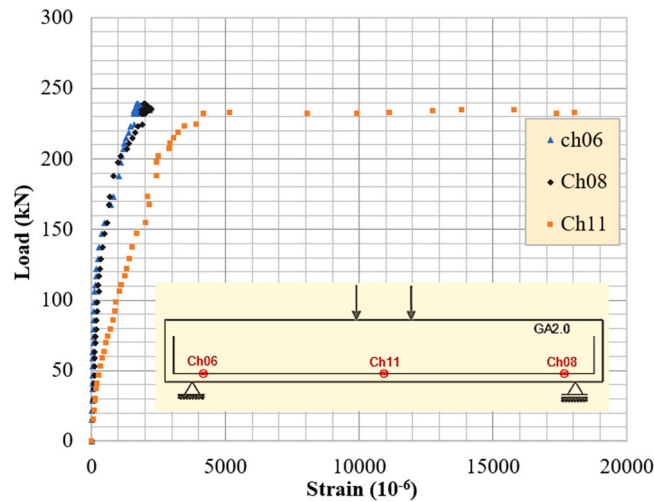


Fig. 18. Load-strain curves obtained from the rebars of the GA2.0.

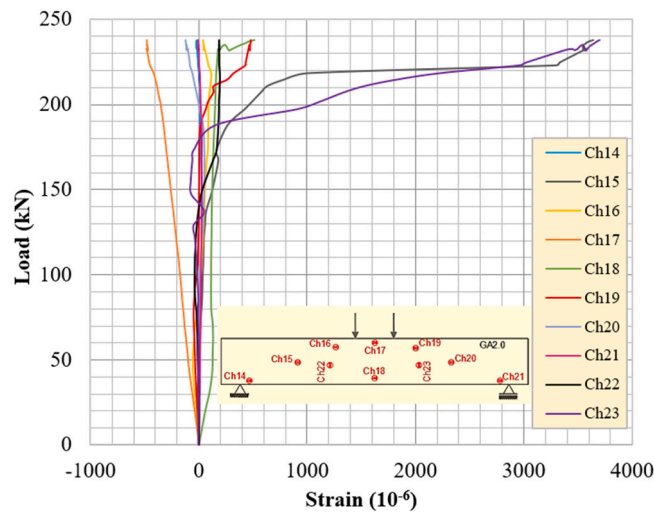


Fig. 19. Load-strain curves obtained from the GA-IHC.

Figs. 22 and 23 relate the load-deflection curves for the rebars and the CG-IHC, respectively.

4. Results and discussion

Data from the experimental studies have been analyzed and compared with previous literature in this section of the study. First, the results are controlled in terms of an examination of the bearing abilities of the beams, and an examination of the maximum loads obtained from the experimental studies. Maximum load capacity reached 216.572 kN in AC2.0, 229.572 kN in CG2.0, and 239.230 kN in GA2.0, determining 4.36%, 10.62%, and 15.28% increases, respectively, compare to the RC2.0. Compared with the reference beam, the RC2.0, the load carrying capacity of the reinforced beams increased by 4% for the AC2.0, 15% for the GA2.0%, and 10% for the CG2.0 (Fig. 24). Based on these increases, the Glass-Aramid hybrid composite (GA-IHC) was the most strengthened and the most effective in terms of maximum load bearing capacity (Fig. 24). Studies in the literature have also found that reinforcement with composite materials increases the load carrying capacity of the RC or concrete beams. For example, Choobbor et al. (2019) [32] emphasized that the increase in the flexural capacity of the strengthened RC beams ranged from 28% to 75% compared to the un-strengthened beam. Similarly, Zhang and Hsu [12] concluded that the epoxy-bonded CFRP increases the load-carrying and shear capacities of the RC beams.

A significant increase in the energy absorption capacity was observed in all beams when the energy absorption capacity was examined. While the energy absorption capacity of the RC2.0 was 10.52 kN.m, the energy absorption capacities of the AC2.0, GA2.0, and CG2.0 were 40.2 kN.m, 11.04 kN.m, and 39.46 kN.m, respectively. It was found that the reinforcement increased the energy

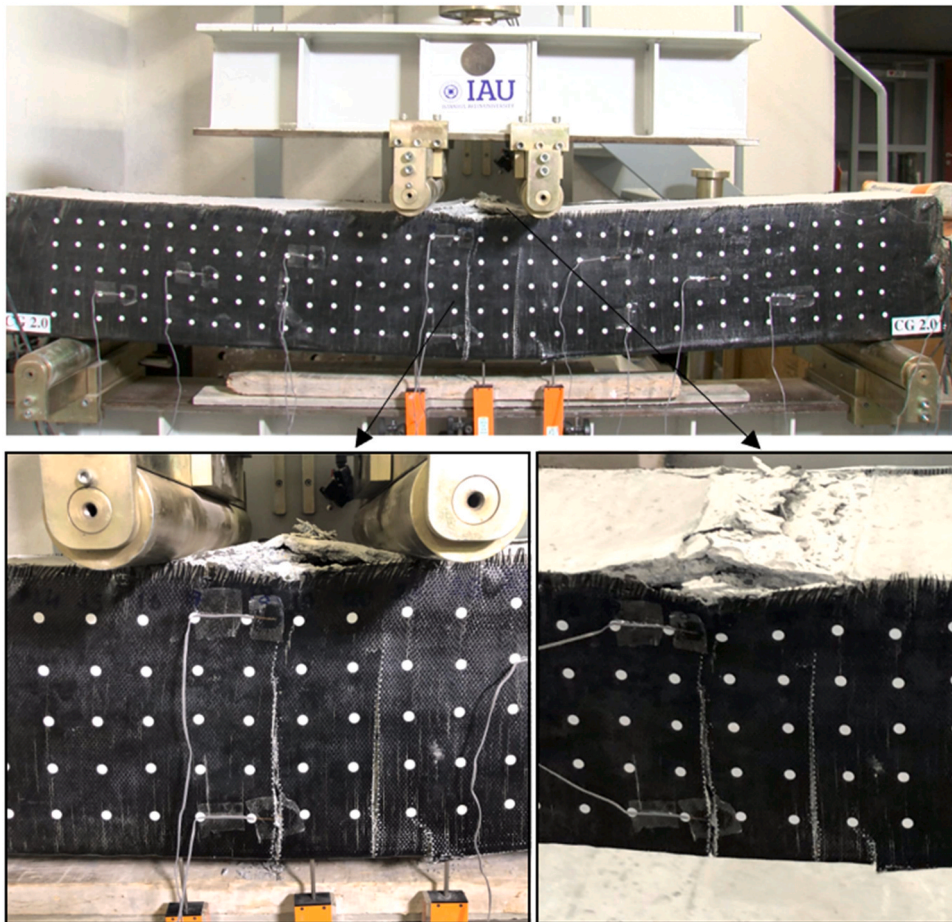


Fig. 20. Crack patterns and failure mode of the CG2.0.

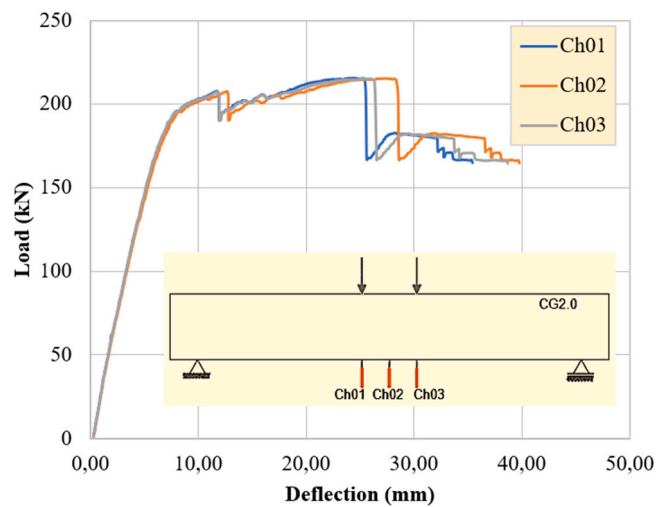


Fig. 21. Load-deflection curves of the CG2.0 beam.

absorption capacity by 382% in AC2.0, 5% in GA2.0% and 375% in CG2.0. It is believed that an increase in beam ductility is the most important factor that contributes to their increased energy absorption capability. This situation has also been emphasized in studies in the literature [33–35].

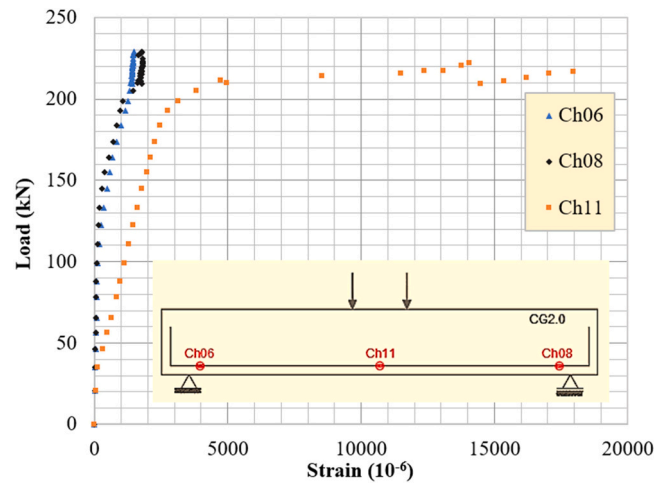


Fig. 22. Load-strain curves obtained from the rebars of the CG2.0.

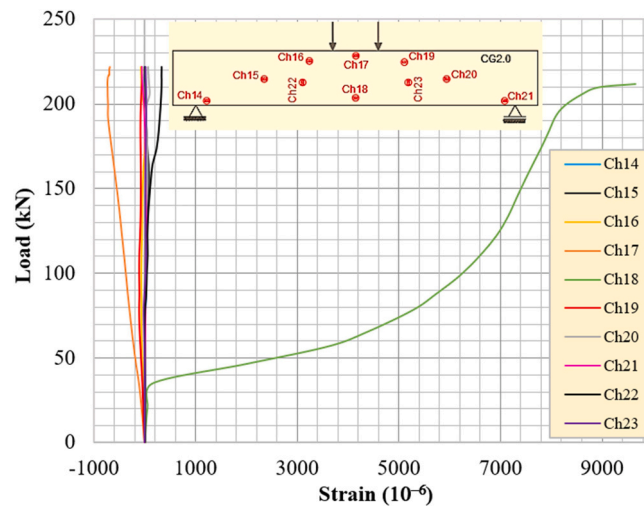


Fig. 23. Load-strain curves obtained from the CG-IHC.

As a part of this study, the deflections at mid-span of each reinforced beam were also compared with the reference beam, RC2.0. A mid-span deflection of the AC2.0, CG2.0, and GA2.0 beams was 40.20 mm, 11.04 mm, and 39.76 mm, respectively, while that of the RC beams was 10.52 mm (Fig. 25). When comparing the maximum deflections, it was found that the GA2.0 and RC2.0 had approximately the same deflection. However, considering the AC2.0 and CG2.0, it was found that the maximum deflections in these beams were about almost 4 times higher than the corresponding deflection of the RC2.0 (Fig. 26). It has been emphasized in many studies in the literature that the maximum displacement capacities of concrete and reinforced concrete beams increase as a result of strengthening with FRP composites. Helal et al. [36] stated that the FRP composites improve the flexural capacity, crack initiation and propagation, stiffness, post cracking behavior, deflection, and ductility of the beams. In addition, Choobbor et al. [32] concluded that the CFRPs and basalt FRPs (BFRPs) improved the deflection capacity of the RC beams.

According to the failure patterns of the beams (Fig. 27), shear failure was prevalent in the RC2.0 beams as expected because the beams were designed with a relatively large bending resistance. Based on the IHC reinforced beams, the failure mode of the GA2.0 was very similar to the RC2.0. However, the failure mode in the GA2.0 beams changed slightly from that of the AC2.0 beams. Rather than failing in shear, these beams failed in flexure. Based on these results, it can be concluded that the AC and CG hybrid composites increase the shear capacity of the beams and cause flexural failure, whereas the GA hybrid composite results in shear fracture due to insufficient increase in shear capacity. It is a very significant contribution that should be taken into consideration. Further, when examining the failure modes, it was found that there was no problem with debonding in any of the beams, and there was a good adhesion and strong bond between the composites and beams, as well. It is important to note that this evidence corroborates the results obtained from many previous studies [20,21,37].

As a result of the strains obtained in the experimental tests, it was found that the strongest strain values for the rebars were recorded

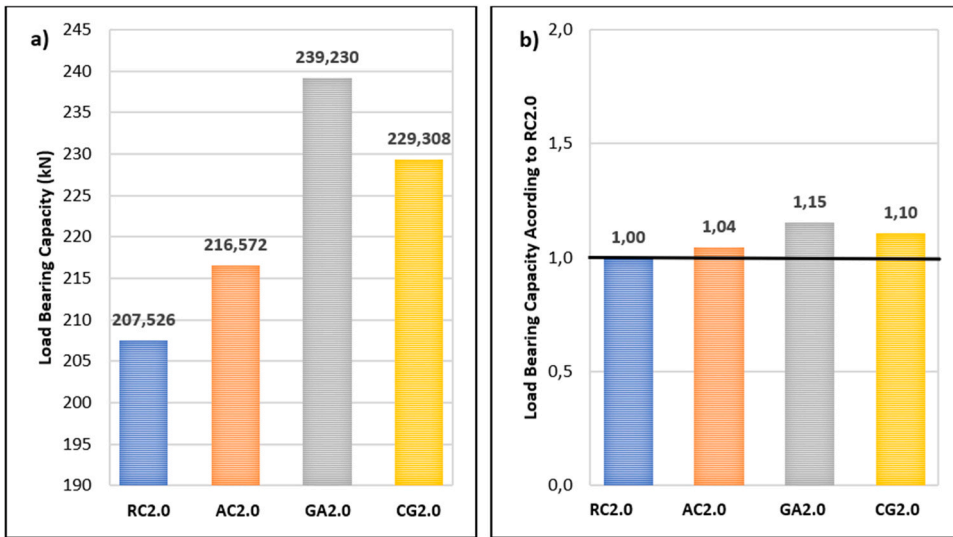


Fig. 24. (a) The load bearing capacities of the beams, (b) the percentage change in load carrying capacities for different strengthening configurations.

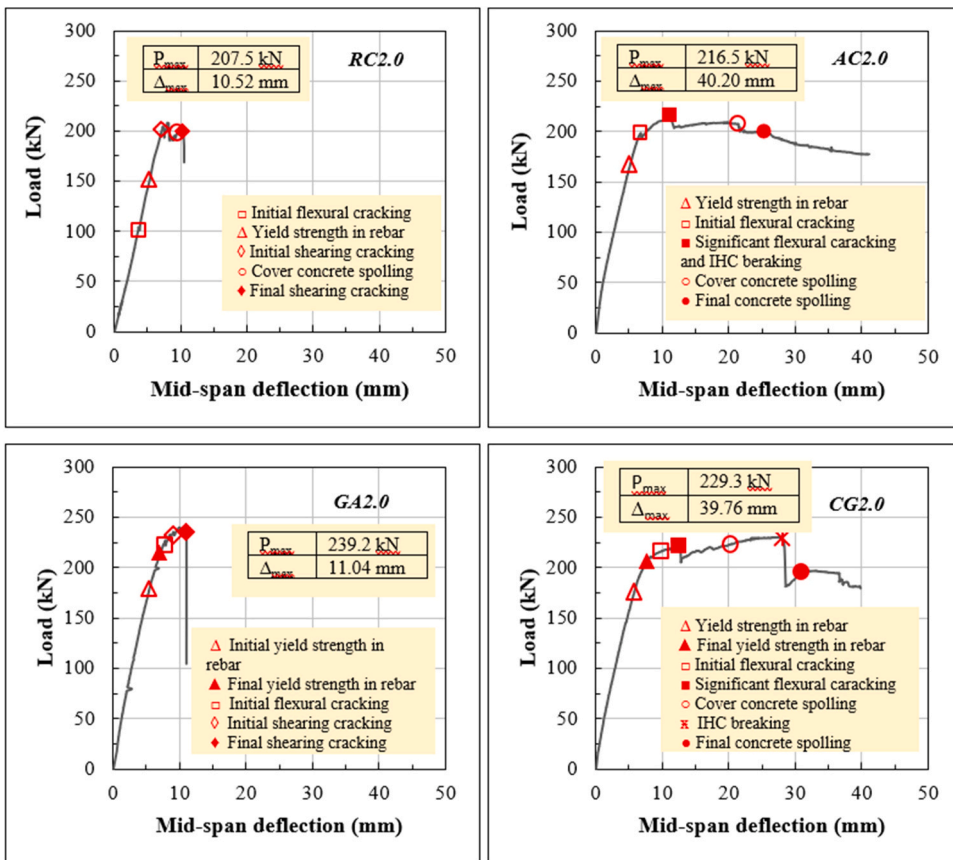


Fig. 25. The maximum deflections at the mid-span of the beams.

using the strain gauges placed in the shear regions of the beams. For the strain gauges installed on RC2.0 longitudinal rebars, yielding was observed to occur primarily in the shear region of the bar located at strain gauge number Ch07. Upon analyzing the strain data of the composites, it was found that the highest strains were measured at the strain gauges that were positioned near the shear regions.

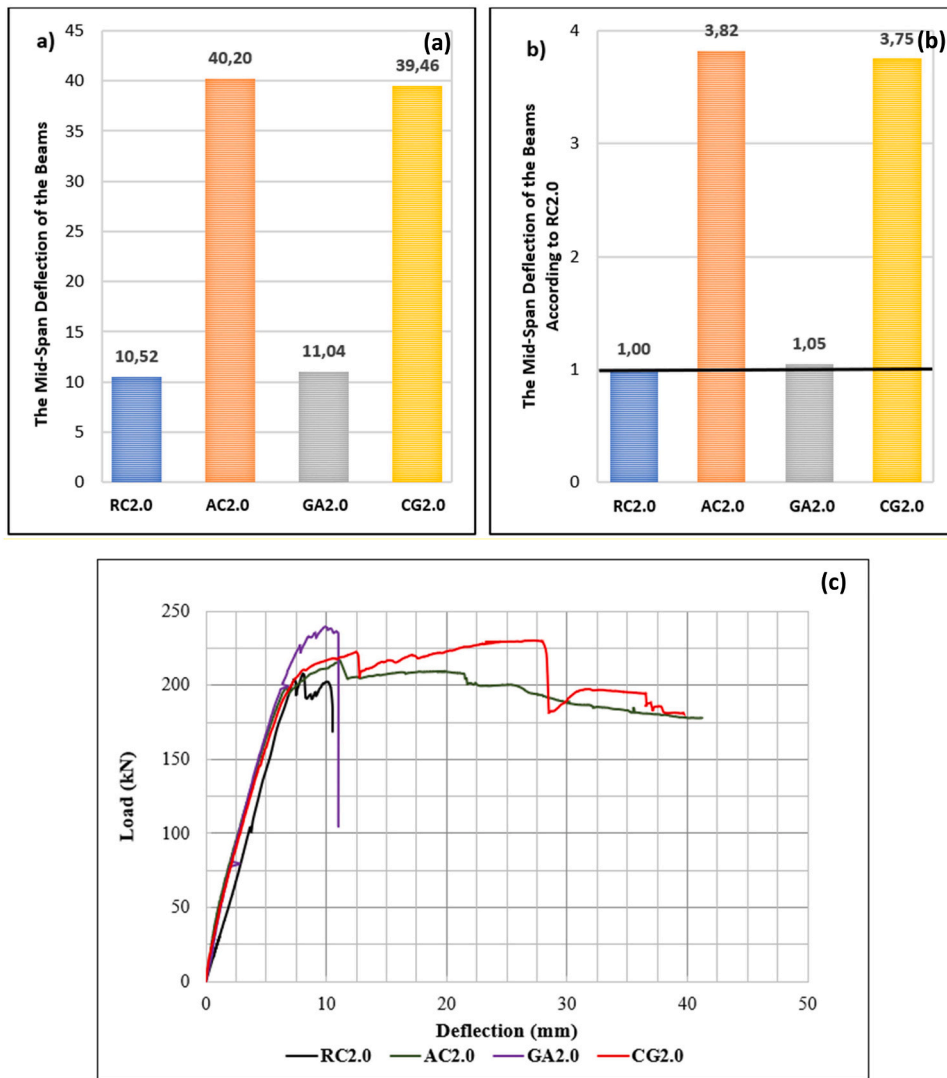


Fig. 26. (a) The mid-span deflection of the beams, (b) the percentage change in mid-span deflections for different strengthening configurations, (c) comparative curve for mid-span deflections.

Taking the example of the AC2.0 beam, the strain data to the maximum strain were recorded by the strain gauge Ch20, located in the shear region. This is an indication that the IHCs contribute positively to the strength of the beams in a state of shear.

5. Conclusion

In recent years, fiber reinforced polymer composites (FRPC) have emerged as one of the most important development groups of materials. It has been observed that the importance of FRPCs has increased in all sectors, and their application in various areas of engineering has improved to a great extent. There are a number of different FRPCs that can now be found in the market today, depending on their application and manufacturing technique. The study focuses on the production of intraply hybrid composites (IHCs), which are made by using two different fibers together.

The main purpose of this study is to investigate the behavior of IHC reinforced beams and the effects of different types of IHC on structural performance. This study investigates the effectiveness of monolayer IHC reinforcement on the RC beams that do not have any transverse reinforcement. As the IHCs, Aramid-Carbon (AC), Glass-Aramid (GA) and Carbon-Glass (CG) are selected. The specimens are then subjected to four-point bending tests under the assumption that the ratio of shear span (a) to effective depth (d) equals 3 ($a/d=3$) and the effects of the IHCs on the strength of the beams are evaluated. From the experimental studies, the following conclusions are drawn:

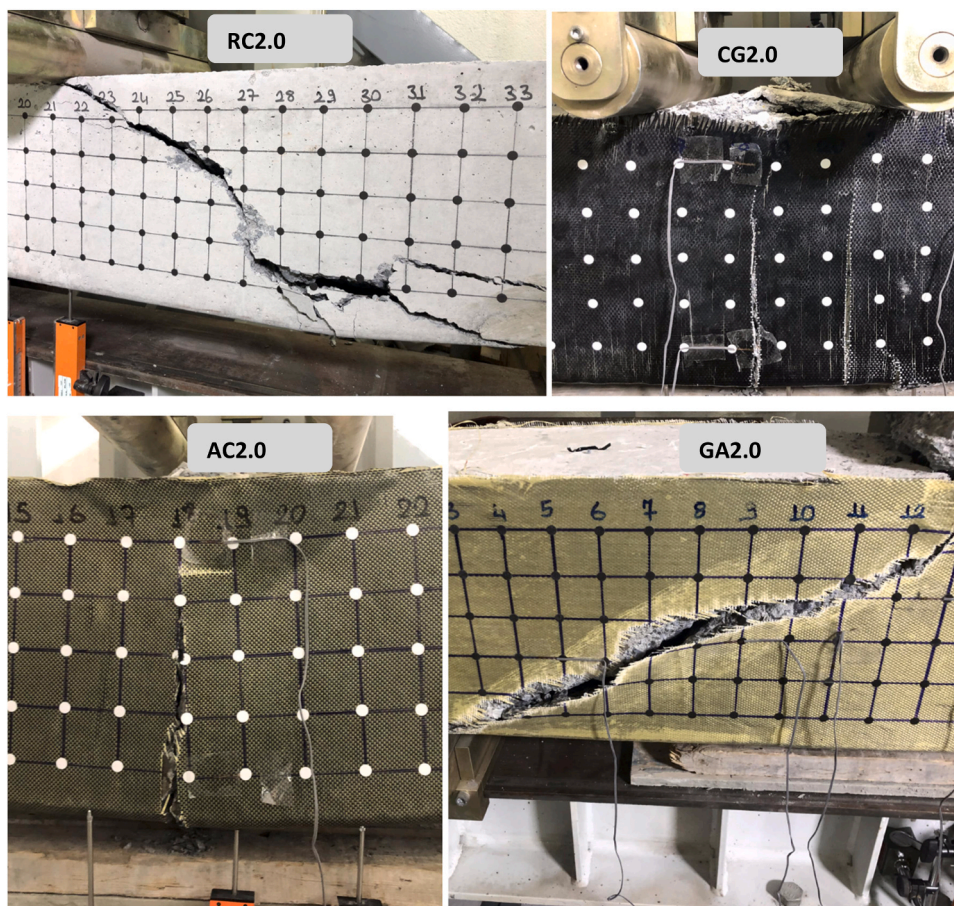


Fig. 27. Failure modes of the beams.

1. In the experimental tests conducted on RC beams, the results showed that the IHCs could play an important role in the structural behavior of the beams. Furthermore, the type of hybrid composite material directly influences the types of failure modes in RC beams as well.
2. After strengthening, the ultimate load capacity reached 216.572 kN in AC2.0, 229.572 kN in CG2.0, and 239.230 kN in GA2.0, representing an increase of 4.36%, 10.62%, and 15.28%, respectively, compared to RC2.0.
3. Considering the energy absorption capacities of the beams, all of the beams have increased their energy absorption after strengthening.
4. A comparison of maximum deflections indicates that the RC2.0 and GA2.0 have similar maximum deflections. However, it is found that the maximum deflections of AC2.0 and CG2.0 are almost four times higher compare to the corresponding values for RC2.0.
5. It is observed that no debonding between the sheets of IHC and the beams exists after the experimental studies. The shear failure mode is eliminated by the AC-IHC and CG-IHC retrofitting.
6. Due to their high performance, ease of application, and innovative design, the IHCs offer excellent and versatile solutions for improving the structural performance of RC structures. Moreover, IHC appears to be the preferred material for a wide range of engineering applications. It should be noted that further studies are needed to better understand the effects of the hybrid composites on the structural behavior of the RC beams considering different dimensions and different a/d ratios of the beams.

Declaration of Competing Interest

The authors declare that they have no known competing financial interests or personal relationships that could have appeared to influence the work reported in this paper.

Acknowledgments

The authors want to acknowledge Prof. Guray Arslan, Prof. Muberra Eser Aydemir and Associate Prof. Cem Aydemir for their assistances in the experimental studies and data elaboration and the technical staff at the Laboratory of Civil Engineering at Istanbul

Aydin University. The financial support provided by the Istanbul Aydin University Scientific Research Projects Center, Turkey through the BAP2019-08 project is gratefully acknowledged.

References

- [1] M.A. Al-Saawani, A.K. El-Sayed, A.I. Al-Negheimish, Effect of shear-span/depth ratio on debonding failures of FRP-strengthened RC beams, *J. Build. Eng.* 32 (2020), 101771, <https://doi.org/10.1016/j.jobbe.2020.101771>.
- [2] A. Siddika, Md.A. Al Mamun, R. Alyousef, Y.H.M. Amran, Strengthening of reinforced concrete beams by using fiber-reinforced polymer composites: a review, *J. Build. Eng.* 25 (2019), 100798, <https://doi.org/10.1016/j.jobbe.2019.100798>.
- [3] I. Shaw, B. Andrawes, Repair of damaged end regions of PC beams using externally bonded FRP shear reinforcement, *Constr. Build. Mater.* 148 (2017) 184–194, <https://doi.org/10.1016/j.conbuildmat.2017.05.077>.
- [4] M.I. Ary, T.H.K. Kang, Shear-strengthening of reinforced & prestressed concrete beams using FRP: Part I – review of previous research!Abstract, *Int. J. Concr. Struct. Mater.* 6 (1) (2012) 41–47, <https://doi.org/10.1007/s40069-012-0004-1>. (doi:).
- [5] J.H. Ha, N.H. Yi, J.K. Choi, J.H.J. Kim, Experimental study on hybrid CFRP-PU strengthening effect on RC panels under blast loading, *Compos. Struct.* 93 (2011) 2070–2082, <https://doi.org/10.1016/j.compstruct.2011.02.014>.
- [6] D. Baggio, K. Soudki, M. Noël, Strengthening of shear critical RC beams with various FRP systems, *Constr. Build. Mater.* 66 (2014) 634–644, <https://doi.org/10.1016/j.conbuildmat.2014.05.097>.
- [7] Z. Wu, X. Wang, K. Iwashita, T. Sasaki, Y. Hamaguchi, Tensile fatigue behaviour of FRP and hybrid FRP sheets, *Compos. Part B: Eng.* 41 (5) (2010) 396–402, <https://doi.org/10.1016/j.compositesb.2010.02.001>. (doi:).
- [8] R.H. Haddad, R.Z. Al-Rousan, B.Kh Al-Sedyri, Repair of shear-deficient and sulfate-damaged reinforced concrete beams using FRP composites, *Eng. Struct.* 56 (2013) 228–238, <https://doi.org/10.1016/j.engstruct.2013.05.007>.
- [9] N. Spinella, Modeling of shear behavior of reinforced concrete beams strengthened with FRP, *Compos. Struct.* 215 (2019) 351–364.
- [10] M.A. Colalillo, S.A. Sheikh, Behavior of shear-critical reinforced concrete beams strengthened with fiber-reinforced polymer-analytical method, *ACI Struct. J.* 111 (6) (2014) 1385.
- [11] A. Boussselham, O. Chaallal, Experimental investigations on the influence of size on the performance of RC T-beams retrofitted in shear with CFRP fabrics, *Eng. Struct.* 56 (2013) 1070–1079.
- [12] Z. Zhang, C.T.T. Hsu, Shear strengthening of reinforced concrete beams using carbon-fiber-reinforced polymer laminates, *J. Compos. Constr.* 9 (2005) 158–169.
- [13] Ç. Uzay, D.C. Acer, N. Geren, Impact strength of interply and intraply hybrid laminates based on carbon-aramid/epoxy composites, *Eur. Mech. Sci.* 3 (1) (2019) 1–5, <https://doi.org/10.26701/ems.384440>. (doi:).
- [14] A. Rajpurohit, S. Joannés, V. Singery, P. Sanial, L. Laiarinandrasana, Hybrid effect in in-plane loading of carbon/glass fibre based inter- and intraply hybrid composites, *J. Compos. Sci.* 4 (2020) 6, <https://doi.org/10.3390/jcs4010006>.
- [15] Y. Zhao, M. Cao, H. Tan, M. Ridha, T. Tay, Hybrid woven carbon-Dyneema composites under drop-weight and steel ball impact, *Compos. Struct.* 236 (2020), 111811, <https://doi.org/10.1016/j.compstruct.2019.111811>.
- [16] N. Hashim, D.L.A. Majid, E.S. Mahdi, R. Zahari, N. Yidrisa, Effect of fiber loading directions on the low cycle fatigue of intraply carbon-Kevlar reinforced epoxy hybrid composites, *Compos. Struct.* 212 (2019) 476–483, <https://doi.org/10.1016/j.compstruct.2019.01.036>.
- [17] B.R. Rajasekar, R. Asokan, M. Senbagan, R. Karthika, K. Sivajyothi, N. Sharma, Evaluation on mechanical properties of intra-ply hybrid carbon-aramid/epoxy composite laminates, *Mater. Today: Proc.* 5 (2018) 25323–25330, <https://doi.org/10.1016/j.matpr.2018.10.335>.
- [18] B. Yang, Z. Wang, L. Zhou, J. Zhang, W. Liang, Experimental and numerical investigation of interply hybrid composites based on woven fabrics and PCBT resin subjected to low-velocity impact, *Compos. Struct.* 132 (2015) 464–476, <https://doi.org/10.1016/j.compstruct.2015.05.069>.
- [19] M.T. Dehkordi, H. Nosrati, M.M. Shokrieh, G. Minak, D. Ghelli, The influence of hybridization on impact damage behavior and residual compression strength of intraply basalt/nylon hybrid composites, *Mater. Des.* 43 (2013) 283–290, <https://doi.org/10.1016/j.matdes.2012.07.005>.
- [20] S. Panchacharam, A. Belarbi, Torsional behavior of reinforced concrete beams strengthened with FRP composites. In First FIB Congress, Osaka, Japan, Vol. 1, 2002: pp. 01–110.
- [21] A. Belarbi, B. Acun, FRP systems in shear strengthening of reinforced concrete structures, *Proc. Eng.* 57 (2013) 2–8.
- [22] ASTM D3039/D3039M-17, Standard Test Method for Tensile Properties of Polymer Matrix Composite Materials, ASTM, West Conshohocken, PA.
- [23] ASTM D792-20, Standard test methods for density and specific gravity (relative density) of plastics by displacement, ASTM, West Conshohocken, PA.
- [24] BS EN 12390-3, Testing Hardened Concrete – Compressive strength of Test Specimens, British Standards Institution, London, UK, 2019.
- [25] BS EN 206:2013+A2, Concrete. Specification, Performance, Production and Conformity, British Standards Institution, London, UK, 2021.
- [26] ASTM C469/C469M-14, Standard Test Method for Static Modulus of Elasticity and Poisson's Ratio of Concrete in Compression, ASTM, West Conshohocken, PA.
- [27] BS EN 12390-5:2019, Testing Hardened Concrete – Flexural Strength of Test Specimens, British Standards Institution, London, UK, 2019.
- [28] BS EN 12390-13:2021, Testing Hardened Concrete – Determination of Secant Modulus of Elasticity in Compression, British Standards Institution, London, UK, 2021.
- [29] ISO 15630-1:2019, Steel for the Reinforcement and Prestressing of Concrete – Test Methods – Part 1: Reinforcing Bars, Rods and Wire, International Organization for Standardization, Geneva, Switzerland, 2019.
- [30] ISO 6892-1:2019, Metallic Materials – Tensile Testing – Part 1: Method of Test at Room Temperature, International Organization for Standardization, Geneva, Switzerland, 2019.
- [31] BS EN 12390-5:2019, Testing Hardened Concrete – Flexural Strength of Test Specimens, British Standards Institution, London, UK, 2019.
- [32] S.S. Choobbor, R.A. Hawileh, A. Abu-Obeidah, J.A. Abdalla, Performance of hybrid carbon and basalt FRP sheets in strengthening concrete beams in flexure, *Compos. Struct.* 227 (2019), 111337.
- [33] H. Jafarzadeh, M. Nematzadeh, Evaluation of post-heating flexural behavior of steel fiber-reinforced high-strength concrete beams reinforced with FRP bars: experimental and analytical results, *Eng. Struct.* 225 (2020), 111292.
- [34] O. Gunes, D. Lau, C. Tuakta, O. Büyüköztürk, Ductility of FRP-concrete systems: investigations at different length scales, *Constr. Build. Mater.* 49 (2013) 915–925.
- [35] C.G. Karayannis, G.M. Sirkelis, Strengthening and rehabilitation of RC beam-column joints using carbon-FRP jacketing and epoxy resin injection, *Earthq. Eng. Struct. Dyn.* 37 (5) (2018) 769–790.
- [36] K. Helal, S. Yehia, R. Hawileh, J. Abdalla, Performance of preloaded CFRP-strengthened fiber reinforced concrete beams, *Compos. Struct.* 244 (2020), 112262.
- [37] G. Ma, H. Li, J. Wang, Experimental study of the seismic behavior of an earthquake-damaged reinforced concrete frame structure retrofitted with basalt fiber-reinforced polymer, *J. Compos. Constr.* 17 (6) (2013), 04013002.

Ferit Cakir^{a,*}, Volkan Acar^b, M. Raci Aydin^c, Bora Aksar^d, Pinar Yildirim^{e,1}

^a Dept. of Civil Eng., Gebze Technical University, Kocaeli, Turkey

^b Dept. of Mechanical Engineering, Ataturk University, Erzurum, Turkey

^c Dept. of Mechanical Engineering, Iğdır University, Iğdır, Turkey

^d Dept. of Civil Engineering, Isik University, Istanbul, Turkey

^e Dept. of Civil Engineering, Istanbul Aydin University, Turkey

* Corresponding author.
E-mail address: cakirf@gtu.edu.tr (F. Cakir).

¹ Ph.D Student, Dept. of Civil Engineering, Istanbul University, Istanbul, Turkey.